I&EC research
Industrial & Engineering Chemistry Research

pubs.acs.org/IECR
Article

Autonomous Flow Control by a Responsive Poly(2-hydroxyethyl acrylate) Organogel-Valve during the Aerobic Oxidation of Benzyl Alcohol

Published as part of Industrial & Engineering Chemistry Research special issue "Smart Reactors—Towards Adaptive, Resilient, and Autonomous Process Systems".

Jonah Hasse, Johannes Gmeiner, Gerrit A. Luinstra,* and Andreas Liese

Cite This: https://doi.org/10.1021/acs.iecr.6c00936

ABSTRACT: Macroscopic poly(2-hydroxyethyl acrylate) organogel beads were synthesized and applied as a chemoresponsive component in a smart valve. Monodisperse round beads of about 3 mm diameter were obtained by cryogenic dripping and subsequent UV photopolymerization of the frozen aqueous monomer solution. The synthesis yields dimensionally stable, soft spheres with a macroporous architecture. The elastic modulus increases from the soft, swollen state in benzyl alcohol to over 250 kPa for high-density networks in the collapsed state in benzaldehyde. They have a degree of swelling in benzaldehyde lower by a factor of 3−7 to that in benzyl alcohol, in dependence of the amount of polyethylene glycol diacrylate cross-linker in the precursor solution. Upon exposure to benzaldehyde, the beads become opaque, indicating a phase transition. Kinetic analysis of the bead volume change for swelling in benzyl alcohol and shrinkage in benzaldehyde gives half-life times in the range of 2−5 min. Beads exhibiting a macroscopic volume change of up to 71% were confined in a casing and acted as a smart valve in a reactor system. The aerobic oxidation of benzyl alcohol to benzaldehyde with a TEMPOL/copper acetate catalyst mixture demonstrated the high efficiency and practical applicability of the self-regulating flow-control component.

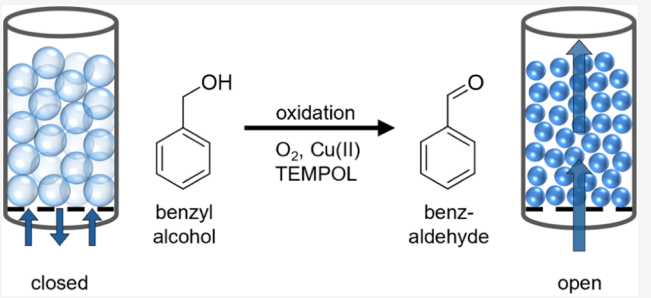

1. INTRODUCTION

The transition in the chemical industry toward renewable feedstocks challenges the operational stability of the established chemical value chains. Biomass-derived raw materials exhibit variable compositions depending on harvest conditions and biological origin.[1] Conventional chemical plants, in contrast, mostly operate effectively under steady-state conditions designed for a constant quality of fossil chemical inputs.[2] This operational rigidity leads to inefficiencies and/or safety risks under more dynamic input loads.[3] Solar and wind power generation introduces further volatility on short timescales in the form of energy supply.[4,5] The implementation of adaptive process systems, therefore, requires a fundamental redesign of control strategies to effectively manage such fluctuations. Resilience has become a primary design criterion for the next generation of chemical reactors and their operation.[6−9]

Intrinsic material-based responses in a chemical production context can offer a robust alternative to external control systems.[10,11] Smart reactors utilize the physicochemical properties of materials for autonomous self-regulation.[8,12] Such an effective decentralization of the process control reduces the dependence on complex hierarchies of electronic sensors and actuators. Stimuli-responsive polymer gels can take the role of direct transducers of chemical information into macroscopic mechanical work.[13] This may take the form of a change in volume, e.g., following a phase transition induced by a trigger.[14] A gel-based actuator then can regulate residence time or flow paths.[15] This principle gives an inherent actuator that is independent of external power sources, detection, or signals.[10,12] Beyond passive flow regulation, the versatility of these materials enables actions such as autonomous pumping[16,17] or fluid sorting,[10,18,19] and even chemical logic gates can be constructed.[20,21]

The application of responsive gels in chemical engineering faces the challenge of "smart material" availability for

Received: March 4, 2026
Revised: April 25, 2026
Accepted: May 29, 2026

https://doi.org/10.1021/acs.iecr.6c00936
Ind. Eng. Chem. Res. XXXX, XXX, XXX−XXX

(commercially) relevant reactions. Today's developments of responsive materials mostly concern aqueous hydrogels for biomedical[22−29] or microfluidic[10,12,30−32] applications.[33−35] In contrast, most industrial chemical syntheses are performed in (dry) organic environments: a plethora of industrial oxidations, esterifications, or polymerizations proceed in organic solvents.[36−39] A multitude of complex transformations also necessitates these solvents for heat transfer and solubility.[40,41] In contrast, sustainable process design increasingly favors solvent-free conditions.[42,43] Actuators should not only be compatible with latter conditions but also exhibit a functionally relevant, i.e., smart, response to critical process variations, like those occurring in the progress of a chemical process.[44−46] The transfer of smart reactor concepts to chemical production in the context of organogels requires new materials with specific solvating properties of organic compounds, i.e., educts and products.[47] The material design must address the compatibility with them. However, only a few studies report on the behavior of responsive gels in nonaqueous environments with relevance to process engineering.[9,46−48]

In addition, kinetic limitations may hinder the implementation of nonporous or closed-cell organogels in macroscopic reactor components.[49] Mass transfer within a dense polymer network then relies on the relatively slow Fickian diffusion.[50,51] The characteristic time of swelling scales with the square of the critical dimension, according to Tanaka's theory of gel kinetics.[50] An actuator with a diameter of several millimeters would require hours to reach an equilibrium of its volume. This slow response prevents the compensation of dynamic process disturbances in real-time.[12] Effective process control necessitates reaction times in the range of seconds or minutes as a compromise.[49,52] A functional actuator thus would combine a useful degree of swelling/shrinkage with high temporal resolution and, on top, should be mechanically robust under the specific flow conditions.

Round organogel beads effectively withstand mechanical stress under flow conditions.[53,54] The regular surface structure promotes a uniform interaction with the surrounding medium.[55] This geometry suits the application as a valve component in cylindrical reactor channels. Spherical geometry ensures a uniform and isotropic response to external stimuli from all spatial directions, and isotropic expansion ensures reliable sealing without complex orientation requirements.[56]

The synthesis of such round, and preferably monodisperse, macroscopic organogel beads constitutes a specific technical challenge. A spherical geometry requires stabilization throughout the entire liquid-to-solid transition during preparation from monomers in order to prevent deformation.[57] Sedimentation polymerization in an immiscible phase offers one established route for such geometries.[58] Surface tension forces shape the liquid monomer solution into a sphere during its descent through a column.[59] However, this technique is critically dependent on the polymerization rate. The droplet must solidify chemically before reaching the bottom of the reactor.[58] This requirement limits the applicability of fast-curing organogel formulations, thereby imposing a significant practical constraint.

Cryogenic fixation decouples the shaping process from the chemical-curing reaction.[60] The procedure comprises the dropwise addition of a monomer solution into liquid nitrogen. The spherical geometry freezes upon impact: physical solidification preserves the shape, and polymerization can be subsequently induced. This separation of morphology control and polymerization in the frozen state expands the choice of the monomers and initiators. The procedure allows us to even use slow-curing organogel formulations for the preparation of spheres.

This study establishes round beads of a simple macroporous organogel as actuators in the bulk synthesis of benzaldehyde from benzyl alcohol. The smart material is primarily based on 2-hydroxyethyl acrylate (HEA) networks. Poly(2-hydroxyethyl acrylate) (PHEA) has been studied in the form of bulk hydrogels[61−63] or coatings;[64,65] however, to the best of our knowledge, no reports were found on macroscopic PHEA-organogel spheres. In addition, the application of structurally defined PHEA beads as intrinsic actuators shifts the focus from passive swelling matrices to active flow-control devices, here in a nonaqueous reactor system. Variations in the resin formulation allowed us to prepare several modifications, each with its characteristic degree of swelling and distinct kinetics of swelling-shrinkage in benzyl alcohol/benzaldehyde. The material system demonstrates a reversible shape change in response to the chemical environment on the scale of minutes. The beads were successfully used to monitor and regulate a reactor system in which the aerobic oxidation of bulk benzyl alcohol to benzaldehyde was carried out. The interplay of high cross-linking density and specific network architecture ensures the mechanical integrity required for effective flow control. This autonomous functionality substantiates the suitability of these beads as intrinsic valve components in resilient, self-regulating chemical reactor systems.

2. EXPERIMENTAL SECTION

2.1. Materials

Benzaldehyde ≥ 99% (Sigma Aldrich, 82024 Taufkirchen, Germany), benzyl alcohol ≥ 99% (Carl Roth, 76231 Karlsruhe, Germany), copper(II)acetate 98% (BLD Pharmatech, 21465 Reinbek, Germany), 4-dimethylaminopyridine 99% (ABCR GmbH, 76187, Karlsruhe, Germany), dimethyl sulfoxide-d_6 (Deutero GmbH, 56288 Kastellaun, Germany), 2-hydroxyethyl acrylate 96% (Sigma Aldrich, 82024 Taufkirchen, Germany), 4-hydroxy-2,2,6,6-tetramethylpiperidin-1-oxyl (TEMPOL, Evonik Industries, 45128 Essen, Germany), lithium-phenyl-2,4,6-trimethylbenzoylphosphinate 98% (TPO-Li, BLD Pharmatech, 21465 Reinbek, Germany), *N*,*N*′-methylene bisacrylamide ≥ 98% (BIS; Sigma Aldrich, 82024 Taufkirchen, Germany), nitrogen (Linde GmbH, 82049 Pullach, Germany), poly(ethylene glycol) diacrylate (PEGDA; Mn of 575 g/mol, Sigma Aldrich, 82024 Taufkirchen, Germany).

2.2. Synthesis of Gel Beads

The protocol for HEA-20 is given as exemplary: 2-hydroxyethyl acrylate (HEA) was dissolved in deionized water to achieve a concentration of 20 wt%. Poly(ethylene glycol) diacrylate (PEGDA) was added as a cross-linker at 0.5 wt%. The photoinitiator TPO-Li was added in an amount of 0.1 wt%. The well-mixed solution underwent ultrasonification for 30 min for degassing. This precursor solution was added dropwise into a bath of liquid nitrogen from a height of approximately 10 cm using a syringe pump (LSP02-1B, Longer Precision Pump Co., Ltd.) equipped with a needle or flexible tubing. The pump rates were 0.06, 0.08, or 0.15 mL·min^{-1} for tubing inner diameters of 0.57, 0.66, and 4.0 mm, respectively. Dispensing of the precursor solution into the liquid nitrogen took 1−3 h, depending on the amount. The precursor solution remained protected from light during that time. Its viscosity showed no observable change during the dripping stage, indicating the absence of polymerization. The frozen droplets were collected from the liquid nitrogen and rapidly transferred to a UV-curing chamber (LED CUBE 100 IC, Hoenle AG (365 nm)[66]). Polymerization was triggered by irradiating the round solid ice beads at a wavelength of 365 nm for 10 min at an

https://doi.org/10.1021/acs.iecr.6c00936
Ind. Eng. Chem. Res. XXXX, XXX, XXX−XXX

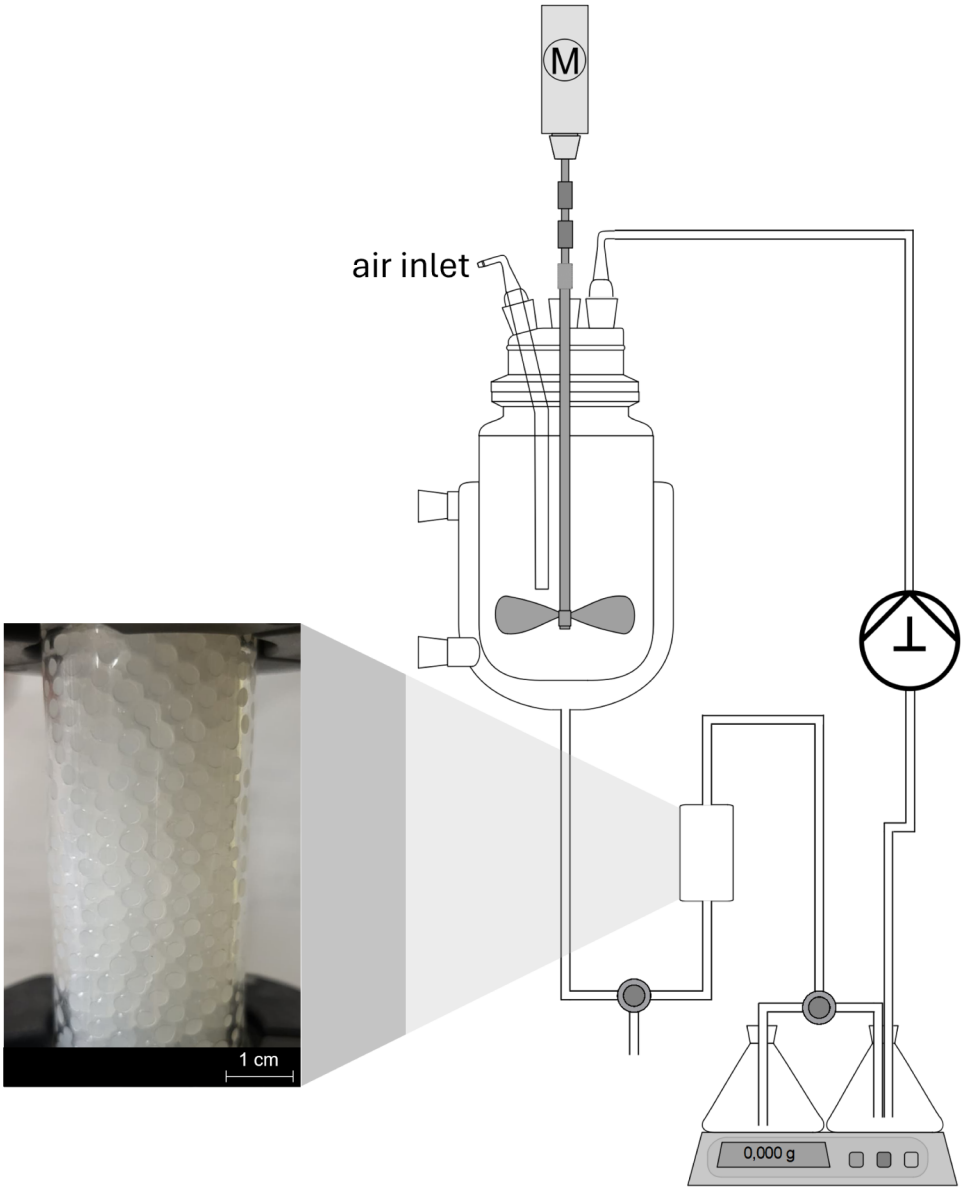

Figure 1. Loop reactor setup for the oxidation reaction; image showing HEA-20 beads (collapsed in benzaldehyde) in a glass casing functioning as a smart valve.

intensity of 880 mW cm^{-2}, at a distance of approximately 15 cm from the light source. The liquid-nitrogen-frozen droplets maintained their solid state and spherical shape during handling for a span below 10 min. The inherent low temperature prevented thawing during polymerization after the irradiation. The resulting beads comprise the water from the precursor solution. They were stored before further processing at −32 °C to minimize solvent evaporation and structural relaxation. The storage time varied between a few days and a few weeks without a noticeable change to the state directly after synthesis. The solvent exchange from water of synthesis to benzyl alcohol was effectuated by thawing the beads (at room temperature) and subsequent immersion in 150 mL benzyl alcohol for at least 24 h. The benzyl alcohol swollen beads were the precursors for benzaldehyde swollen beads. Therefore, these were kept in benzaldehyde for another 24 h.

2.3. Size Distribution

The particle size distribution of the as-synthesized organogel beads was determined by using optical imaging. A picture of a statistical population of more than 100 beads was acquired by using a digital camera (CANON EOS R50, Canon Germany GmbH). The macroscopic bead diameters were quantified by digital image analysis using the open-source software ImageJ (version 1.54g).

2.4. Swelling Properties

2.4.1. Gravimetric Degree of Swelling. The dry mass m_{dry} of the beads was set to the mass of the lyophilized cryogel beads (obtained at −90 °C, 0.250 mbar, 48 h using a Gamma 2-16 LSCplus freeze-dryer (Osterode am Harz, Germany)). The mass of the swollen beads $m_{swollen}$ was obtained after removing excess surface liquid from the beads that had been immersed in benzyl alcohol or benzaldehyde for 48 h. The equilibrium degree of swelling (DoS) was calculated as the ratio of $m_{swollen}$ and m_{dry}.

2.4.2. Optical Measurement Setup and Determination of Swelling Rates. Preswollen beads in benzyl alcohol or benzaldehyde were mounted on a thin metal skewer within a glass cuvette using a 3D-printed lid to fix their position. The cuvette was filled with the complementary compound to induce medium exchange inside the beads. Changes in bead dimensions were monitored by using a digital camera (CANON EOS R50, Canon Germany GmbH) with an image capture interval of 30 s. The resulting image series were analyzed using a Python script (utilizing OpenCV) for the detection of the

https://doi.org/10.1021/acs.iecr.6c00936
Ind. Eng. Chem. Res. XXXX, XXX, XXX−XXX

Table 1. Composition of Precursor Solution Leading to Organogel Beads

organogel	monomer (wt%)	cross-linker (wt%)	dosing end diameter (mm)	DoS in benzyl alcohol	DoS in benz-aldehyde
HEA-10	HEA (10)	PEGDA (0.5)	0.66	45 ± 4	10 ± 1
HEA-20-0	HEA (20)	– (0)	0.66	19 ± 2	3.7 ± 0.5
HEA-20	HEA (20)	PEGDA (0.5)	0.66	21 ± 3	4.0 ± 0.6
HEA-40	HEA (40)	PEGDA (0.5)	0.66	10.8 ± 0.4	1.9 ± 0.1
HEA-20-2	HEA (20)	PEGDA (2.0)	0.66	15.0 ± 0.9	5.3 ± 0.4
HEA-20S	HEA (20)	PEGDA (0.5)	0.57	26 ± 2	5.0 ± 0.3
HEA-20L	HEA (20)	PEGDA (0.5)	4.0	23.8 ± 0.5	5.0 ± 0.2
HEA-20BIS	HEA (20)	BIS[a]	0.66	22.9 ± 0.7	3.4 ± 0.2

[a]Equimolar to 0.5 wt% of PEGDA.

bead boundaries. The bead diameter was calculated from the rounded boundary. Cyclic switching was performed by alternating the exposure of the beads for 30 min to benzaldehyde or benzyl alcohol. Five cycles were completed while tracking the diameter. The solvent sensitivity was assessed by exposing the beads to binary mixtures (10 mL) of benzyl alcohol and benzaldehyde (0, 25, 50, 75, and 100 vol%). The beads were equilibrated in each mixture for 45 min before their diameter was recorded.

2.5. Mechanical Properties

Compression tests were carried out using a rheometer (Discovery HR 30, TA Instruments) equipped with a parallel plate geometry (diameter of 25 mm). Individual beads equilibrated in benzyl alcohol or benzaldehyde were placed centrally on the lower plate. A standard gap zeroing was performed prior to loading: the upper plate was manually positioned in close proximity to the sample apex. Subsequently, an axial compression ramp was applied at a speed of 50 μm/s up to a maximum strain of 50%. For each formulation and solvent condition, at least five independent replicates were measured. The Young's modulus E was calculated from the force-displacement curves by fitting the Hertzian contact model for spherical objects $F = 4/3 \cdot E/(1 - \nu^2) \cdot \sqrt{R \cdot \delta^3}$, where F is the normal force, R is the bead radius, ν is the Poisson ratio, and δ is the displacement.[67,68] The Poisson's ratio was set to 0.5.

2.6. Scanning Electron Microscopy (SEM)

The gel beads were examined using scanning electron microscopy (LEO Electron Microscopy Inc., One Zeiss Drive, Thornwood, NY 10594, USA). Water-swollen samples were lyophilized prior to imaging (Gamma 2-16 LSCplus, Osterode am Harz, Germany). The dried samples were fractured to expose the interior and were coated with a thin layer of carbon. Images were acquired at an acceleration voltage of 5.0 kV.

2.7. Valve Testing System

An autonomous loop reaction system was built around a 500 mL double-walled glass reactor with a central bottom outlet (Figure 1). Agitation of the reaction medium was ensured by an electronic overhead stirrer (IKA EUROSTAR digital, Staufen, Germany) utilizing a propeller rotating at 1300 rpm. Compressed air was sparged into the reaction solution using a custom-fabricated glass tube equipped with a sintered glass frit (porosity 1) to ensure fine bubble dispersion. The smart valve consisted of a custom-fabricated glass housing (height 70 mm, inner diameter 25 mm), which facilitated the direct optical monitoring of the organogel volume phase transition. The organogel beads were filled into this casing and were retained there by a chemically inert stainless steel mesh (1 mm mesh size).

The reaction mixture was allowed to leave the main reactor at the bottom and was directed to flow through the organogel valve from the bottom to the top to prevent compaction and clogging. The effluent then entered a collection container placed on a precision balance (Mettler Toledo, Giessen, Germany). A diaphragm metering pump (ProMinent Delta optoDrive, Heidelberg, Germany) with a maximum flow rate of 30 $L \cdot h^{-1}$ continuously recirculated the reaction mixture back to the main reactor. A software-based proportional-integral (PI) control algorithm adjusted the pump stroke frequency in real-time to maintain a constant mass in the collector vessel. The pump frequency correlated directly with the valve throughput, serving as a flow meter for the system. The entire process automation and data logging were executed by a LabManager system (LM-LABBM2B, HiTec Zang GmbH, Herzogenrath, Germany).

2.8. General Procedure for Benzyl Alcohol Oxidation

A stock solution was prepared by dissolving copper(II) acetate (1 mol %) and 4-dimethylaminopyridine (DMAP, 2 mol%) in 350 mL of benzyl alcohol. This mixture was stirred for 16 h at room temperature to ensure the dissolution of all components. Five minutes prior to the reaction start, TEMPOL (1 mol%) catalyst was added to the solution. The smart valve assembly had been loaded with organogel beads that were equilibrated in benzaldehyde for 30 min to reach the collapsed state. The reactor was filled with the reaction mixture, and the recirculation pump was activated to establish a feedback loop. The oxidation was initiated by commencing the admission of compressed air into the reactor vessel. Reaction progress was monitored by taking samples and evaluating their ^{1}H NMR spectra (Bruker 300 MHz spectrometer) (Figure S1; cf. SI): aliquots of the reaction mixture (0.1 mL) were withdrawn and diluted with DMSO-d_6. The molar conversion was quantified by integrating the signals of the methylene protons of benzyl alcohol and calculating the ratio relative to the intensity of the aldehyde proton signal of benzaldehyde.

3. RESULTS AND DISCUSSION

3.1. Synthesis and Morphological Characterization of "Smart HEA-Beads"

Poly(2-hydroxyethyl acrylate) (PHEA) was chosen as the matrix material for its nonionic and nonthermoresponsive properties. PHEA does not undergo a phase transition upon changing the temperature, which allows for the investigation of solvent interactions without thermal interference.[69,70] The high density of hydroxyl groups in PHEA gives the option of hydrogen bonding, which is the strongest interaction in organic systems with heteroatoms.[71] A differentiation of the interactions of PHEA with various organic compounds then becomes more likely. The reported selective TEMPOL-catalytic oxidation of benzyl alcohol to benzaldehyde using oxygen from air was selected here as a model reaction for the conversion of benzyl alcohol educt to benzaldehyde.[72] The smart gel would need to switch the valve whenever the oxidation reaches completion. The latter may also be relevant for preventing overoxidation.

Different interactions of the polymer making up the organogel beads with benzyl alcohol and benzaldehyde are of central importance to this study. These can be estimated from the Hansen solubility parameter concept, wherein an interaction distance R_a is calculated based on established group contribution methods (Table S1).[73] The R_a values of PHEA for benzyl alcohol and benzaldehyde indeed are quite different:[74] benzyl alcohol has a small R_a value of 6.6 $MPa^{0.5}$

https://doi.org/10.1021/acs.iecr.6c00936
Ind. Eng. Chem. Res. XXXX, XXX, XXX−XXX

(Table S2), typical for a high solvent quality. Benzaldehyde, in contrast, shows a significantly larger R_a value of 13.8 $MPa^{0.5}$, indicative of a solvent of much lower quality.

Beads of PHEA in the range of 0.25−0.50 cm were prepared using a cryogenic free-radical polymerization technique starting from HEA solutions in water. Dropping a precursor monomer solution into liquid nitrogen immediately fixes the spherical geometry of the droplets. A consecutive UV initiation of the polymerization in the frozen state preserves the isotropic distribution of the monomers. Conversion of the monomers seems complete by IR analysis, and the presence of a sol fraction was not investigated. The chemical uniformity of the synthesized beads provides a well-defined model system for systematically investigating the influence of cross-linker density on the swelling characteristics. The approach circumvents the need for a dispersive phase or emulsifiers, which are typically required in the case of conventionally synthesized gel beads in suspension polymerization procedures.[75,76]

The HEA was mostly cross-linked with small amounts of polyethylene glycol diacrylate (PEGDA) to yield macroreticular materials (Table 1; 0.5 wt% in the precursor solution). A systematic approach is adopted for an easy identification of the beads, relating them to the composition of the precursor solution. A prefix HEA is followed by the wt% of HEA in the solution, which is followed by a dash to denote the amount of PEGDA if the latter is different from 0.5 wt%. Extensions S for small or L for large refer to an inner diameter of the dispensing tube other than 0.66 mm and BIS for the substitution of PEGDA as a cross-linker. The cryogenic droplet protocol can be applied to a broader variation of monomers. The synthesis also yielded dimensionally stable beads of *N*-isopropylacrylamide (NiPAAm) and HEA-NiPAAm copolymers, which will be reported upon later. Notably, dimensionally stable particles from the HEA monomer were even formed in the absence of a chemical cross-linker. This stability suggests that during polymerization, sufficient self-cross-linking reactions occur to achieve the spherical integrity after thawing. Consequently, the cryofreezing step effectively ensures the topological fixation that led to complex macromolecular architectures after UV curing.

The cryogenic dropping technique also yields dimensionally stable spherical organogel beads of similar size (Figure 2). Variation of the tubing inner diameter at the end of the dosing line directly controls the final particle size. The dry density of the beads thus scales with the mass of the monomers in the droplets. The number # of the HEA-# bead thus also is an indicator of the polymer density. The particle sizes of the beads from the smallest tubing are monomodal and normally distributed with a mean close to 0.3 cm (HEA-20S/HEA-20; Figure 3). The dripping process is known to produce highly uniform droplets at small diameters; however, shock-freezing in liquid nitrogen becomes a limiting factor when the droplets are formed from 4 mm tubing. Beads formed in this execution appear to be bimodally distributed (HEA-20L). A close examination of the freezing of the larger droplets in the liquid nitrogen bath reveals that the impact occasionally leads to the ejection and formation of small satellite droplets. The impact-induced splashing upon contact with the liquid nitrogen surface is hard to avoid. The resulting distribution can be adequately described by two normal distributions with a similar mean (within 10%). These beads still pack into a dense ensemble, which is a useful feature for valves based on stacked beads.[77,78]

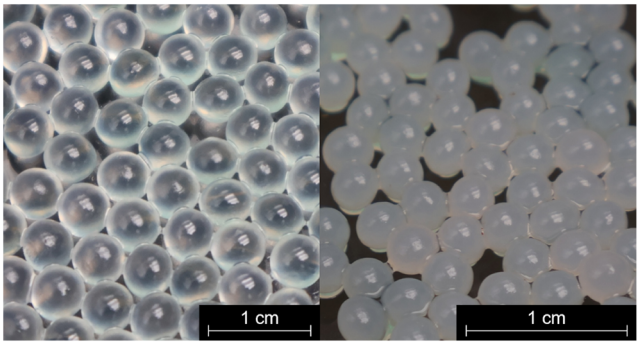

Figure 2. Organogel beads of HEA-20 after swelling in benzyl alcohol (left) and benzaldehyde (right; not at the same scale).

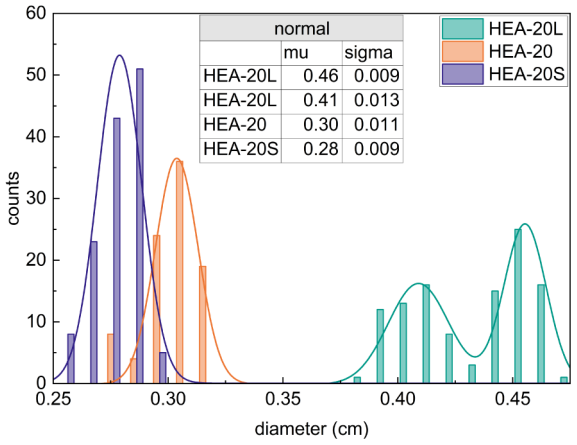

Figure 3. Size distribution (diameter) with Gaussian fit of the gel beads after synthesis.

Scanning electron microscopy (SEM) reveals the macroporous network structure within the lyophilized beads (Figure 4). It is important to note that the PHEA network has a glass-transition temperature close to ambient conditions (10−15 °C),[64,79] rendering the solvent-free polymer rubbery and tacky at room temperature. This soft state inevitably allows for some viscoelastic relaxation and shrinkage during lyophilization. The micrographs, however, confirm that an open-cellular structure is present, as expected.

The most elaborated HEA-20 system displays a sponge-like topology with unevenly distributed pores. The pore structure provides sufficient free volume for solvent uptake, correlating with the high equilibrium degree of swelling (DoS of 21 ± 3) in benzyl alcohol. The HEA-40 sample with a lower concentration of cross-linker in the polymer has significantly thicker polymer walls between the pores. The effective cross-linking per bead is higher (less pores lead to a lower surface-to-volume ratio), a lower mobility of chain segments results, and a higher stress arises in the material upon swelling. This restricts the swelling capacity to about 50% of that of HEA-20 (Table 1). The structure of HEA-20-0 (no cross-linker) also shows a high(er) thickness of the polymer walls. The inner surface appears quasi-continuous and punctured with pores rather than a fibrous network. Polymerization of the monomer is accompanied by a volumetric shrinkage, and at low cross-linking densities, a flow can occur during network formation, leading to partial collapse of the rubbery polymer structure.

https://doi.org/10.1021/acs.iecr.6c00936
Ind. Eng. Chem. Res. XXXX, XXX, XXX−XXX

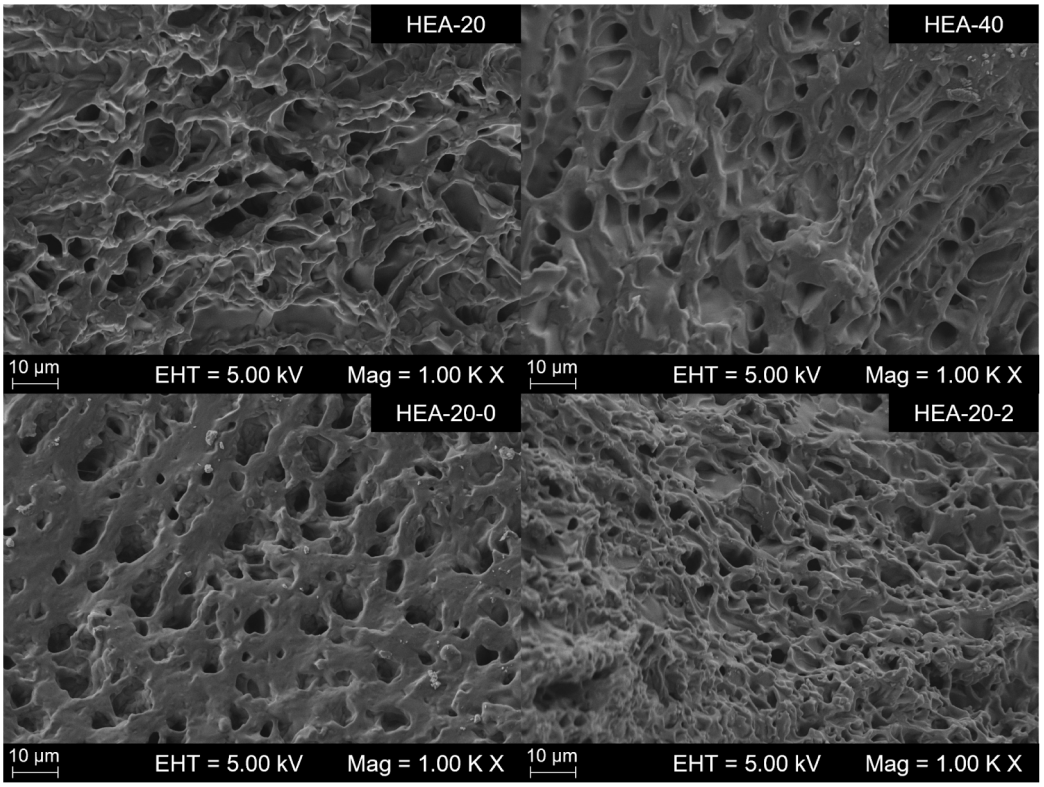

Figure 4. SEM images of the internal structure of freeze-dried hydrogel beads (HEA-20, HEA-40, HEA-20-0, and HEA-20-2).

Higher PEGDA concentrations accelerate the macroscopic gelation. Rapid network formation promotes the phase separation of the polymer chains from the aqueous phase.[80] This kinetic restriction generates a finer network architecture with smaller pore dimensions. HEA-20-2 has a denser microstructure than that of HEA-20. The high number of cross-links creates a denser polymer mesh with restricted mobility: a degree of swelling (DoS) in benzyl alcohol of only 15.0 results, and the difference in DoS in benzyl alcohol and benzaldehyde is only a factor of 3 instead of about 5 with 0.5 wt% of PEGDA (and 6−7 for BIS) or no PEGDA in the precursor solution (*vide infra*).

3.2. Mechanical Properties and Elastic Modulus

The macroscopic stiffness of the organogel beads was quantified using unconfined compression testing on single beads (Figure S2). The elastic force is a central quality in the kinetics of swelling and shrinkage and therefore of interest.[81] The data show a nonlinear response $F \propto \delta^{1.5}$ in the low-deformation regime lower than a 10% strain, which is expected for a Hertzian contact model of spherical geometries. Regression analysis confirmed the validity of the Hertzian fit for small compressive loads, indicating a predominantly elastic response. The mechanical stiffness of the beads correlates directly with the solvent-dependent chain conformation (Figure 5).[82,83] The expanded network in benzyl alcohol means a high chain mobility of coils between cross-links and gives a low macroscopic stiffness to the bead. The polymer chains collapse to contracted globule aggregates to minimize solvent contact in benzaldehyde. This densification restricts segmental mobility and increases the number of effective load-bearing segments per unit volume, transforming the material into a rigid solid. This appears as a favorable property for a packed ensemble of beads confined to the casing of the valve,

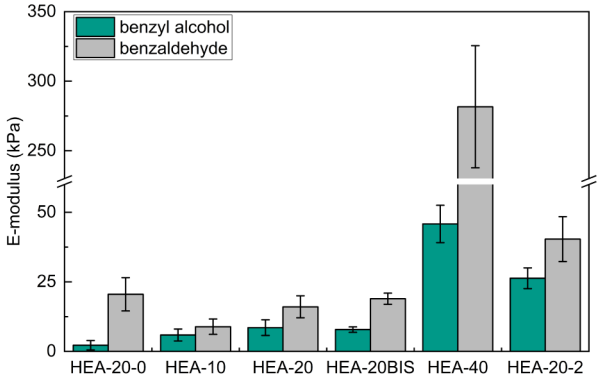

Figure 5. Elastic modulus of organogel beads in benzyl alcohol and benzaldehyde at 10% compression.

lowering the propensity of irreversible fusion of beads (Figure 1).

The stiffness follows the polymer density, but no simple numerical dependencies arise (the cross-linker concentration in the polymer is varying too). The HEA-10 formulation, having the lowest monomer concentration, exhibits the lowest modulus in the HEA-# series with 0.5 wt% of PEGDA. The highest increase in rigidity is observed for HEA-40, reaching values exceeding 250 kPa in the collapsed state. The beads contain the most mass of polymer per unit volume, thus reaching the highest density of load-bearing polymer segments. The difference between the swollen state with little mechanical resistance and the collapsed state is thus the highest.

A higher concentration of cross-linker leads to a higher stiffness in the bead, mostly noticeable in the collapsed state. HEA-20BIS has comparable mechanical properties to HEA-20, the shorter cross-linker only tending to have somewhat better

https://doi.org/10.1021/acs.iecr.6c00936
Ind. Eng. Chem. Res. XXXX, XXX, XXX−XXX

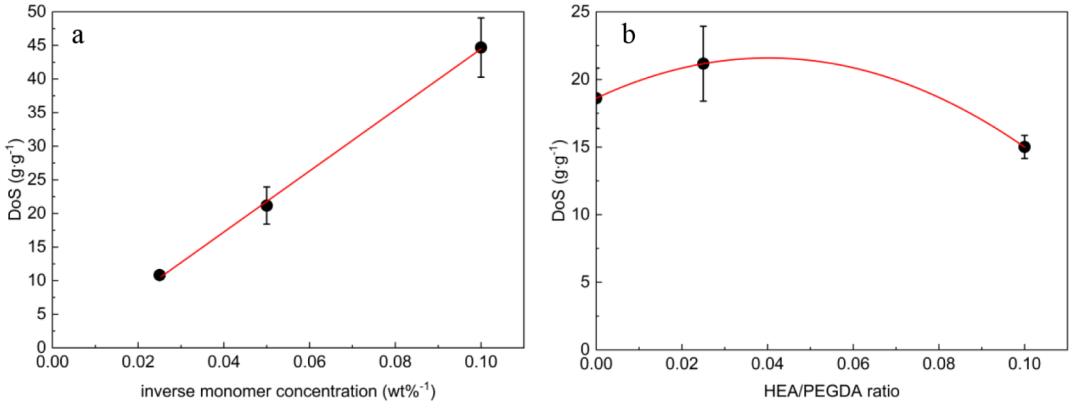

Figure 6. DoS of beads in benzyl alcohol as function of (a) HEA-# (# = 10, 20, 40) and (b) PEGDA content (HEA-20-0, ..., 2).

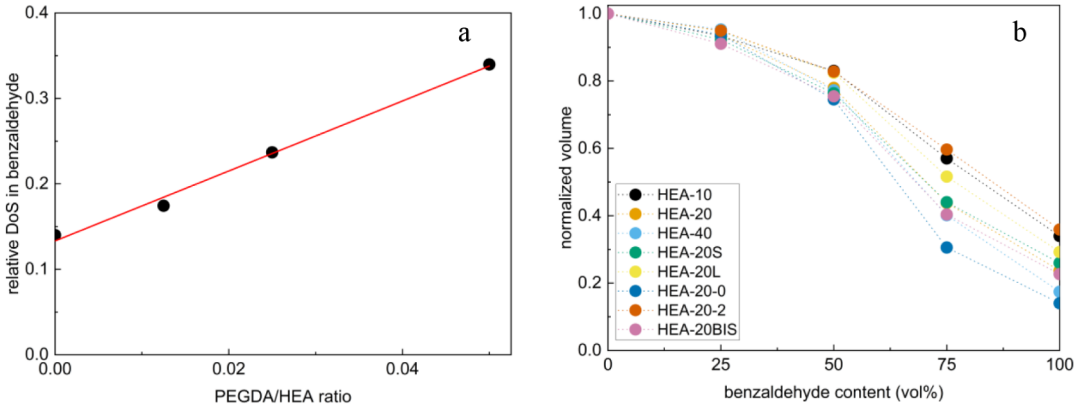

Figure 7. (a) Relative volume of beads in benzaldehyde as function of PEGDA content; (b) relative bead volume as a function of the solvent composition.

mechanical properties. Furthermore, beads with 6.6 mm (HEA-20L) and 3.8 mm (HEA-20S) diameters have no significant differences in the elastic modulus. This demonstrates that a homogeneous gel has formed in the cryo-droplet method of synthesis. This also confirms that the mechanical response is an intrinsic material property and not an artifact of the macroscopic sample geometry.

3.3. Swelling Behavior and Solvent Kinetics in Benzyl Alcohol–Benzaldehyde System

3.3.1. Equilibrium Swelling. The DoS (mass of the swollen bead in relation to the mass of the polymer) of the beads was determined gravimetrically in both benzaldehyde and benzyl alcohol. The swelling in benzyl alcohol leads to substantially clear organogels (Figure 2). Benzyl alcohol is the better solvent, and all organogels reach their individual maximum volume in it (Table 1). The DoS in benzyl alcohol is proportional to the inverse of the HEA monomer content in the precursor solution (Figure 6), making the product of monomer content and DoS, i.e., the $m_{swollen}$, almost a constant with a value of 445−455. The higher concentration of the polymer chain segments in the beads of comparable size (*vide infra*) exerts a higher osmotic driving force for solvent uptake (dilution). The higher elastic forces of the network counteract further expansion to balance this osmotic pressure, ultimately limiting the hydrodynamic volume to a nearly constant value for these formulations.[81]

The DoS in benzyl alcohol appears only weakly dependent on the concentration (or even presence) of the chemical cross-linker (Figure 6b). Beads prepared without a cross-linking agent have, within error limits, the same DoS as the formulations with 0.5 wt% PEGDA cross-linker. Free-radical acrylate polymerizations inherently undergo intermolecular chain transfer reactions. These transfer events abstract tertiary protons from the polymer backbone and create midchain radicals. The midchain radicals initiate long-chain branching and subsequent chemical self-cross-linking.[84,85] A chemical cross-linker (PEGDA) introduces further covalent anchor points. The low PEGDA concentration alters the predominant baseline network only slightly. Increasing its content to 2.0 wt % (1:10 to HEA), thereby increasing the solid content, gives a bit more than the expected lower DoS on account of the mass. A network with higher elastic forces is indicated, which is congruent with the mechanical property profiles. The choice of BIS as a cross-linker (using 20 wt% of HEA) also gives beads with properties very comparable to HEA-20.

Subsequent submersion in benzaldehyde shrinks the macroscopic beads, and they become opaque (Figure 2). The poor solvent quality drives the polymer segments to interact and leads to solvent expulsion (*vide supra*). The polymer segments separate into a denser phase, which raises the refractive index. The refractive index mismatch between the polymer-rich domains and the surrounding solvent causes the light scattering, which underlies the macroscopically observed turbidity. The distinct swelling behaviors in benzyl alcohol and benzaldehyde may also be understood as a direct consequence of specific interactions. Benzyl alcohol, bearing a hydroxyl group, would form an intermolecular hydrogen bond network with the PHEA segments. These favorable

https://doi.org/10.1021/acs.iecr.6c00936
Ind. Eng. Chem. Res. XXXX, XXX, XXX−XXX

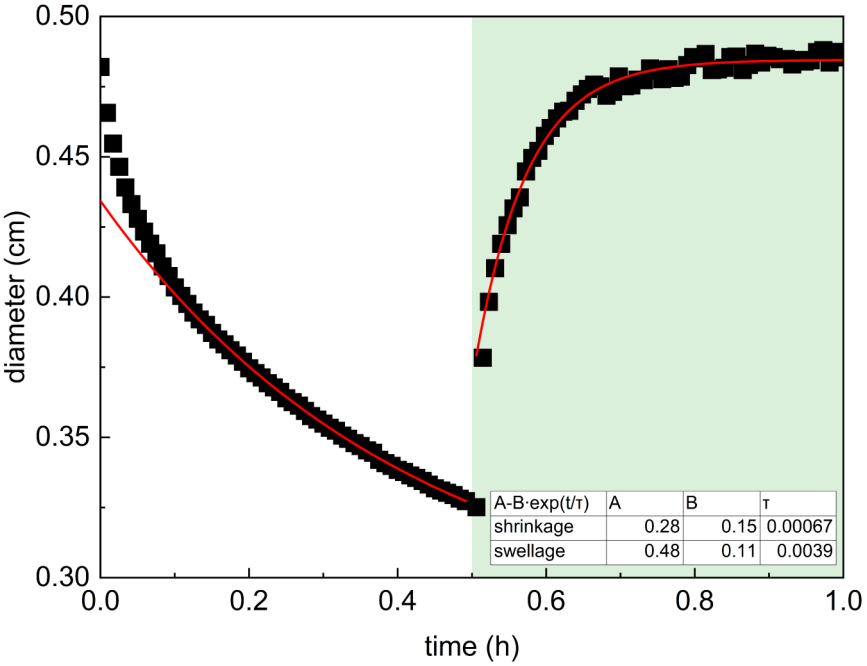

Figure 8. Swelling in benzyl alcohol and shrinkage in benzaldehyde and exponential fit (of the 2nd phase) of HEA-20 beads.

polymer−solvent interactions overcome polymer−polymer interactions, yielding a solvated, expanded network. In contrast, the aldehyde entity of benzaldehyde formally is only a hydrogen bond acceptor. The absence of a corresponding donor moiety renders intra- and intermolecular hydrogen bonding between the PHEA chains thermodynamically more favorable.

Normalization of the individual DoS to their respective swelling in benzyl alcohol reveals that the lower the cross-linker density in the polymer (ratio of cross-linker to monomer), the lower the DoS becomes (Figure 7a). The linear dependence starts for HEA-20-0 at a relative DoS of about 0.15 and increases to 0.34 at an HEA to PEGDA ratio of 20 to 1 (wt:wt) in HEA-10. This indicates that the inherent cross-linking of HEA building blocks during polymerization is of particular importance when, relative to HEA, little PEGDA is used. This is in accordance with the SEM images of the respective networks (Figure 4). The effect levels off at lower HEA to PEGDA ratios: the relative DoS of HEA-20-2 (ratio of 10) is only 0.36, contrasting with the expected 0.54 of a linear extrapolation and is indicative of an appreciably stiffer network. The effect of substitution of PEGDA for BIS again is marginal. Larger HEA-20-based particles show a smaller difference in relative DoS but are still in a similar range of 0.3. This range is more than sufficient for smart valve applications.

The dependence of the relative DoS on the benzaldehyde content in benzyl alcohol is of major importance for a valve that is responsive to the degree of oxidation of benzyl alcohol to benzaldehyde. Depending on the operation of a reactor, a strong response only at high conversion is favored, or, alternatively, a smooth transition during conversion could be used to monitor the progress of the oxidation reaction. The relative DoS of the HEA organogels shows an approximate quadratic decrease (Figures 7b, S3, and Table S3) with the benzaldehyde content. The response is thus an intermediate-strength one. Still, it was decided to use these gels for the construction of a smart valve to show that the concept is viable.

The HEA-20 system has a volume change of 77% from benzyl alcohol to benzaldehyde, a significant variation in the hydrodynamic cross section. Even at 50% of benzaldehyde (corresponding to 50% conversion in a reaction for benzyl alcohol oxidation to benzaldehyde), the relative DoS still is 80%. This shape-change capability enables the beads to act as intrinsic valves within a fluidic channel. The material could thus autonomously regulate the flow path in response to the local chemical environment without the need for external sensors or power sources, provided that the rate of change of the volume is reasonably fast.

3.3.2. Kinetics of Swelling and Shrinkage. The rate of swelling of the beads was addressed within a previously reported setup.[86] The beads were thus mounted on a thin metal skewer and exposed to an organic medium inside a cuvette. Their volume was monitored by taking photographs at preset intervals by using a computer-based controller. The diameter was evaluated from the number of pixels that the bead makes up in a frame using a Python script. Changes of the volume were calculated from the diameter and were related to the degree of swelling (DoS) by assuming a uniform and constant density of the differently swollen beads. The time-dependent diameter in the second phase was fitted to a first-order decay/growth model. The swelling-shrinkage of hydrogel beads has been shown to go through two apparent phases.[87] Both phases can be described by exponential functions. The second, slower phase of the diameter change is probably more characteristic of the network.[81] The time constants (i.e., collective diffusion coefficient)[81] contain contributions of the network's mechanical moduli and the friction factor for solvent exchange.

The experimentally determined diameters d were fitted as $d(t) = A - B\exp(t/\tau)$ with A, B, and τ as fit parameters, minimizing the sum of residuals (Figure 8: the red line is the fit, demonstrating a good agreement to the measurements). Regression analysis consistently yielded high coefficients of determination across all beads, confirming that the macro-

https://doi.org/10.1021/acs.iecr.6c00936
Ind. Eng. Chem. Res. XXXX, XXX, XXX−XXX

Table 2. Swelling and Shrinkage in Benzyl Alcohol Resp. Benzaldehyde

time constants τ (1000 s)	HEA-10	HEA-20	HEA-40	HEA-20-0	HEA-20-2	HEA-20BIS
shrinkage	0.83 ± 0.07	1.1 ± 0.2	1.4 ± 0.2	0.93 ± 0.05	1.7 ± 0.2	1.1 ± 0.1
swelling	0.48 ± 0.04	0.24 ± 0.04	0.33 ± 0.08	0.11 ± 0.01	0.52 ± 0.12	0.34 ± 0.06
diameter swollen d_0 (cm)	0.44	0.48	0.41	0.60	0.42	0.49
ultimate volume change ΔV (%)	61	77	59	81	68	76
volume change 30 min (%)	57	70	52	75	53	69

scopic volume transition follows a predictable exponential behavior in that second phase. Consequently, the derived characteristic time constant τ serves as a robust metric to quantitatively compare the response rates of different network architectures (Table 2). The swelling curve rises significantly faster than the decay of the shrinkage curve, the solvent expulsion with collapse of the chain segments being slower than the expansion (Figure 8). This is a usual feature, the dissolution of the polymer into a good solvent being more rapid.[86]

Fast swelling-shrinkage kinetics constitute a critical feature for the application of the beads inside a smart valve. The valve should preferably react faster than conversion proceeds (here, exemplary of benzyl alcohol to benzaldehyde). The swelling kinetics of the HEA-# (#: 10, 20, 40, 20-0, 20-2, and 20BIS) beads depend on their network architecture. The crucial later phase of swelling of HEA-20 has a time constant of 240 s (corresponding to a half-life of approximately 3 min). The smaller initial swelling phase proceeds significantly faster, and the time constants for the slower extension phase across all formulations range from 110 s (HEA-20-0) to 520 s (HEA-20-2). This temporal resolution means an acceptable lag between the chemical trigger for many reactions and the gel response, implying that a close to real-time process control can be achieved. The shrinkage is about 3 times slower on average, which is also an acceptable value for application in a smart valve for moderately fast reactions (at room temperature).

The macroscopic dimensions of HEA-20 reproducibly oscillate between the swollen and collapsed states (Figure 9)

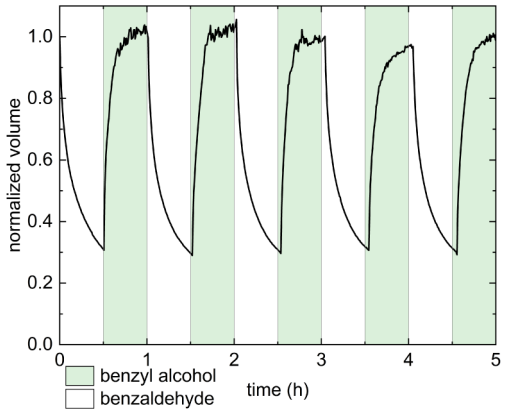

Figure 9. Cyclic exposure (30 min) of HEA-20 beads to benzyl alcohol (green underlay) and benzaldehyde.

upon cyclic exposure to solvents. The higher density of HEA-40 and the more cross-linked HEA-20-2 formulations exhibit a gradual decrease in the swelling capacity over consecutive cycles (Figures S4−S10). This drift indicates a progressive accumulation of kinetically trapped states or plastic deformation and relaxation from the constitution after synthesis within the denser polymer matrix. The HEA-20 gel therefore seemed more useful as a component in a smart valve. The shrinkage to a normalized volume fraction of about 0.3 is very constant, and the swelling reaches mostly the initial values after shrinkage in benzaldehyde. The time constants for swelling and shrinkage are also very constant. This organogel thus withstands the mechanical stress during the response without (immediate) failure, and the network seems robust with no immediate signs of fatigue.

3.4. Application in a Valve for Autonomous Feedback Loop Control

The concept of intrinsic material intelligence was evaluated in a closed-loop circulation reactor using benzaldehyde formed by the aerobic oxidation of benzyl alcohol as the chemical trigger (Figure 1). The beads were arranged in a glass casing with close packing of equal spheres. The valve is not completely sealed by the beads. It is designed to maintain a small leakage flow, ensuring continuous contact between the medium and the beads, even in the swollen state. This flow is necessary to keep (at least parts of) the beads under the same conditions as the reactor content or close to it. Otherwise, the exchange of information between the valve and the reactor will be delayed to a random extent, i.e., beyond that of the response time of the beads. This will, e.g., be the case if the contact of the beads with the reaction medium is only at beads at the surface of the valve. The outflow of the reactor through the valve is collected in a flask, and a pump returns it back to the reactor at about the same rate (*vide supra*).

The oxidation of benzyl alcohol to benzaldehyde uses oxygen as an oxidant and is catalyzed by a previously reported homogeneous mixture of copper(II) acetate (1 mol%), 4-dimethylaminopyridine (DMAP, 2 mol%), and TEMPOL (1 mol%) acting as the radical mediator (Scheme 1).[72] An

Scheme 1. Aerobic Oxidation of Benzyl Alcohol by the TEMPOL/Copper Acetate Catalytic System

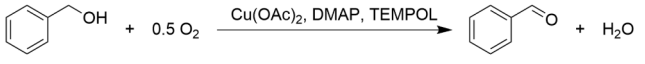

oxidation does not proceed in its absence. The organogel in the valve is also in contact with the components of the catalytic system. A degradation of PHEA by the catalytic system, however, was not obvious. Progressive conversion of benzyl alcohol to benzaldehyde induces the projected shrinkage of the polymer beads.

The initial conditions of the setup had HEA-20 organogel beads in the valve that were equilibrated in benzaldehyde. The solid, collapsed beads were loosely packed in the valve casing, i.e., without any compressive preload, thereby establishing the initially open flow state at the onset of the reaction (Figure 1). This packing procedure turned out to be crucial (*vide infra*). The benzyl alcohol-catalyst mixture was initially added to the collection vessel. The process was started by turning on the

https://doi.org/10.1021/acs.iecr.6c00936
Ind. Eng. Chem. Res. XXXX, XXX, XXX−XXX

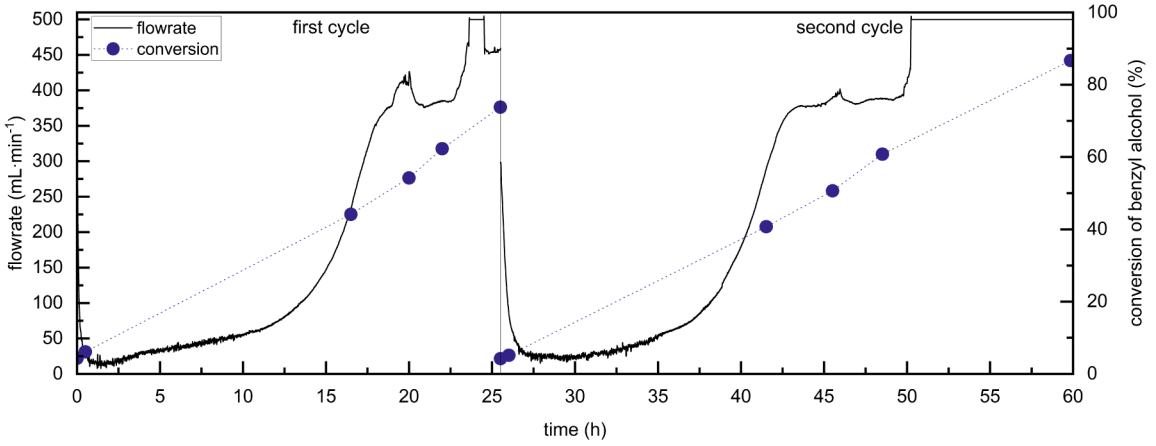

Figure 10. Flow rate and molar conversion of benzyl alcohol in a loosely packed valve system during two cycles (one reloading with benzyl alcohol and catalyst system).

recirculation pump and the air supply. The system's response was characterized by the pump frequency, which serves as a flow meter for the hydrodynamic permeability of the packed bed in the valve. In this setup, the organogel beads function simultaneously as the sensor, processor, and actuator.

Upon initiation of the pump as benzyl alcohol is admitted to the reactor, the loosely packed valve underwent a rapid self-sealing (Figure 10). The flow rate drops within the first few minutes from an initial value of approximately 300 mL·min^{-1} to a baseline level below 20 mL·min^{-1}. This residual permeability is defined as the "closed" state for this reactor configuration. The rapid kinetics of this closure confirm the high solvent sensitivity and the fast response rates observed for the organogel single beads.

The valve maintains this closed state of maximum hydrodynamic resistance for the subsequent 10 h. The catalytic oxidation of benzyl alcohol proceeds steadily, as is evidenced by the spectroscopic analysis of samples. The accumulation of the benzaldehyde product gradually alters the thermodynamic quality of the mixture for swelling the beads. The increasing fraction of benzaldehyde triggers a noticeable shrinkage of the organogel beads at conversions above 40%. This gradual shrinkage facilitates a continuous, sigmoidal recovery of the flow rate (Figure 10). Initially, the confined beads maintain their positions. Extensive shrinkage ultimately eliminates critical interparticle contact points, and the packed bed reorganizes itself. This later-stage macroscopic rearrangement alters the flow channels abruptly. The structural shift produces the observed discontinuous jumps in the flow rate at high conversion. As the conversion reaches 70% after 22 h, the loosely packed valve opens to its largest extent, reaching a flow rate of 400−500 mL·min^{-1}. This permeability change of more than 20-fold demonstrates the successful translation of the chemical transition into a macroscopic process control function.

A consecutive second reaction cycle in the else-unmodified setup showed the reversibility and operational stability of the smart valve. Replacing the product-rich reaction mixture for a fresh benzyl alcohol mixture (after 25.5 h) makes the organogel beads to respond immediately: the flow rate returns to the baseline level of below 20 mL·min^{-1}, resetting the valve to its closed state. As the second oxidation period progressed, the valve maintained this hydrodynamic resistance until the accumulation of benzaldehyde once again triggered the macroscopic shrinkage of the beads. The flow rate mirrored the actuation profile of the first cycle and ultimately reached the fully open state again.

These real-time data provide direct phenomenological evidence of the material's intrinsic intelligence. The synchronous evolution of the hydrodynamic profile with the reaction coordinate confirms that the organogel beads autonomously process the chemical information. The shift in solvent quality is translated into a functional mechanical output, thereby opening the feedback loop without external electronic devices. Repeated cycling confirms that the organogel beads fully retain their solvent responsiveness and structural integrity even under prolonged operational stress (chemically and physically), thereby validating their suitability for multicycle autonomous process control.

It is also found that the actuation profile of the valve is highly dependent on the initial configuration. When the organogel beads are initially subjected to a compressive preload (packed tightly in the casing at the beginning), a distinctly different (and surprising) close-open-close flow profile emerges (Figure 11) in the course of the benzyl alcohol oxidation. Initially, the baseline flow rate is briefly recorded at approximately 200 mL·min^{-1} before the tightly packed beads swell rapidly upon contact with the reaction

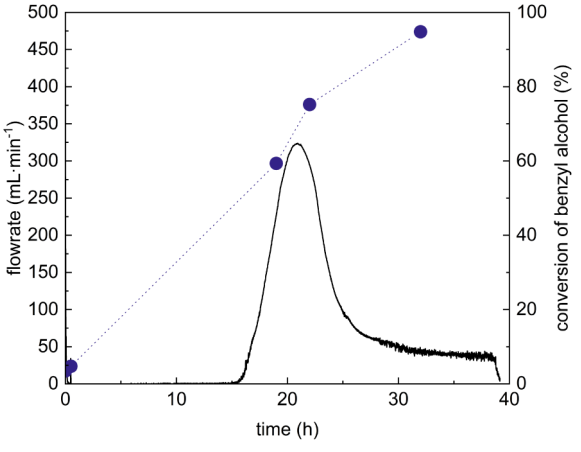

Figure 11. Time-dependent profile of the flow rate and molar conversion of benzyl alcohol in the initially tightly packed valve system.

https://doi.org/10.1021/acs.iecr.6c00936
Ind. Eng. Chem. Res. XXXX, XXX, XXX−XXX

mixture, causing the permeability to plummet within minutes as described above. This creates a tight seal, with the compressed valve allowing no permeation of liquids for the next 15 h. Despite this prolonged and highly restrictive closed state, the continuous accumulation of benzaldehyde eventually triggers a strong structural response. The macroscopic shrinkage of the network overcomes the compressive preload, leading to a steep, robust recovery of the flow rate. The valve opens to reach a maximum flow rate of approximately 325 mL·min^{-1} at 70% conversion. However, as the reaction proceeds further, the flow rate autonomously decreases again, and the valve completely reseals itself.

This secondary closure can be attributed to the formation of water as an equimolar byproduct of the aerobic oxidation of benzyl alcohol. As it turned out, water in benzaldehyde also swells the beads but to a lesser extent than benzyl alcohol (Figure 12). In contrast to a valve with a loosely packed HEA-20, a prominent reduction in flow is observed when the casing is tightly packed with beads. The individual beads are more confined in the tightly packed bed, and the function of the valve changes.

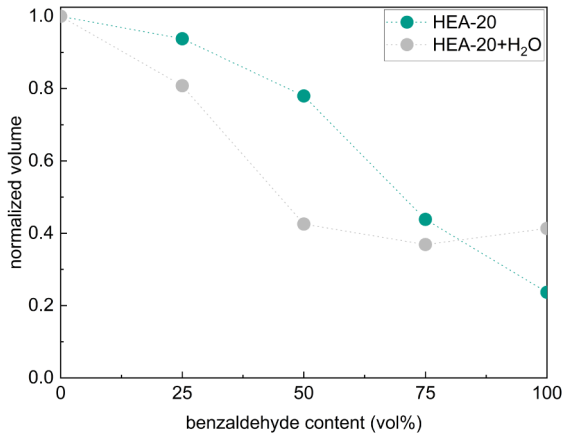

Figure 12. Relative bead volume as a function of the solvent composition in benzyl alcohol/benzaldehyde (HEA-20) and benzyl alcohol/benzaldehyde/water (HEA-20+H_2O).

An experiment simulating the oxidation was conducted on the swelling of the beads to gain this insight, tracking the volume of the HEA-20 beads in solvent mixtures that mimic the increasing water fraction alongside that of benzaldehyde (Figure 12). The ternary system containing water exhibits a significant volume turnaround at high benzaldehyde and water fractions (above 75%). The outcome shows that the presence of water is nontrivial, as it often is in organic media.

Water acts as a strong hydrogen-bond provider to the hydroxyls at the PHEA side chains. Interaction of the aqueous byproduct apparently effectively competes with polymer−polymer interactions that govern the collapsed state in benzaldehyde. A partial hydration and macroscopic reswelling of the gel network result. Consequently, this water-induced volumetric expansion is sufficient to partly eliminate the interstitial voids again when these are small in the tightly packed valve. The reswelling overcomes the initial benzaldehyde-induced shrinkage, autonomously sealing the flow channels at high conversions.

The microstructural changes and mechanical dynamics underlying this multistimuli response surface of the HEA beads remain to be elucidated in future, more systematic investigations.[88] The synthesis of HEA copolymers is an option to tune the thermodynamic potential to the diverse properties of educts and derived products. The outcome also shows that the development of a valve based on smart organogels relies on engineering its constitution and shape in concert with each other.

4. CONCLUSIONS

Cryogenic shaping in combination with free-radical polymerization provides a versatile platform for tailoring macroscopic organogel actuators. The synthesis allows for the precise topological fixation of diverse network architectures to meet specific hydrodynamic requirements. The HEA-based material transitions autonomously from a soft, expanded state, blocking a channel, to a rigid solid upon solvent quality deterioration. This mechanical contrast ensures reliable channel sealing against backpressure and thus could eliminate the need for external sensor-actuator loops. The swelling kinetics are compatible with real-time process control for moderately fast reactions. The mobility of the HEA network enables rapid bead expansion, particularly during an initial swelling. The open pore structure of the beads ensures rapid solvent exchange during switching, thereby overcoming the slow diffusion limitations typical for nonporous gels. The swelling kinetics are primarily governed by the macroscopic bead geometry and porosity rather than the specific molecular architecture of the cross-links. The material has the potential to act as a combined sensor (solvent recognition), a processor (phase transition), and an actuator (volume expansion) within a single structural element. Solvent—i.e., medium-responsive organogels—would be an option for intrinsic material intelligence in chemical engineering. Future (microfluidic) systems may utilize these self-regulating components to dynamically adapt to their chemical environment, reducing the complexity of the peripheral control infrastructure.

■ ASSOCIATED CONTENT

Supporting Information

The Supporting Information is available free of charge at https://pubs.acs.org/doi/10.1021/acs.iecr.6c00936.

Data of the fundamental physicochemical, mechanical, and kinetic characterization of the HEA organogel beads, including raw measurement files (.csv, .xlsx), processed results, and the custom Python script used for automated image analysis, are openly available at https://doi.org/10.15480/882.17264; representative ^{1}H NMR spectrum of the aerobic oxidation reaction mixture (Figure S1); force-displacement curve and Hertzian contact model fit from unconfined compression testing (Figure S2); group contributions for the calculation of the Hansen solubility parameters (Table S1); calculated Hansen solubility parameters and interaction distances for the polymer network and solvents (Table S2); relative bead volume as a function of the solvent composition, including quadratic model fitting (Figure S3, Table S3); cyclic swelling and shrinkage profiles of varying organogel formulations during alternating solvent exposure (Figures S4−S10) (PDF)

https://doi.org/10.1021/acs.iecr.6c00936
Ind. Eng. Chem. Res. XXXX, XXX, XXX−XXX

AUTHOR INFORMATION

Corresponding Author

Gerrit A. Luinstra − *Institute of Technical and Macromolecular Chemistry, University of Hamburg, Hamburg 20146, Germany;* orcid.org/0000-0003-4602-8319; Email: luinstra@chemie.uni-hamburg.de

Authors

Jonah Hasse − *Institute of Technical and Macromolecular Chemistry, University of Hamburg, Hamburg 20146, Germany;* orcid.org/0009-0008-9086-8239

Johannes Gmeiner − *Institute of Technical and Macromolecular Chemistry, University of Hamburg, Hamburg 20146, Germany*

Andreas Liese − *Institute of Technical Biocatalysis, Hamburg University of Technology, Hamburg 21073, Germany;* orcid.org/0000-0002-4867-9935

Complete contact information is available at: https://pubs.acs.org/10.1021/acs.iecr.6c00936

Author Contributions

J.H.: Writing—original draft, Writing—review and editing, Visualization, Validation, Software, Methodology, Investigation, Formal analysis, Data curation, Conceptualization. J.G.: Writing—review and editing. G.A.L.: Writing—review and editing, Methodology, Formal analysis, Supervision, Project administration, Investigation, Funding acquisition, Conceptualization. A.L.: Writing—review and editing.

Notes

The authors declare no competing financial interest.

ACKNOWLEDGMENTS

This project is funded by the Deutsche Forschungsgemeinschaft (DFG, German Research Foundation) − SFB 1615 − 503850735.

REFERENCES

(1) Sheldon, R. A. Green and sustainable manufacture of chemicals from biomass: state of the art. *Green Chem.* **2014**, *16* (3), 950−963.

(2) Keßler, T.; Kienle, A. Robust Design and Operation of a Multistage Reactor for Methanol Synthesis from Renewable Resources. *Processes* **2023**, *11* (10), 2928.

(3) Pistikopoulos, E. N.; Barbosa-Povoa, A.; Lee, J. H.; Misener, R.; Mitsos, A.; Reklaitis, G. V.; Venkatasubramanian, V.; You, F.; Gani, R. Process systems engineering − The generation next? *Comput. Chem. Eng.* **2021**, *147*, 107252.

(4) Cegla, M.; Semrau, R.; Tamagnini, F.; Engell, S. Flexible process operation for electrified chemical plants. *Curr. Opin. Chem. Eng.* **2023**, *39*, 100898.

(5) Loewert, M.; Pfeifer, P. Dynamically Operated Fischer−Tropsch Synthesis in PtL-Part 1: System Response on Intermittent Feed. *ChemEngineering* **2020**, *4* (2), 21.

(6) Vieira, C. S. P.; Malafaia, D.; Cunha, D. R.; Leal, J. F.; António, J. P. M.; Gois, P. M. P.; Garcia-Martinez, J.; Noël, T.; Poliakoff, M. RESILIENCE by design: ten principles to guide chemistry in a volatile world. *Green Chem.* **2025**, *27* (26), 7742−7747.

(7) TUHH *Reactors for Future Process Engineering* https://www.tuhh.de/sfb1615/welcome.

(8) Hu, X.; Karnetzke, J.; Fassbender, M.; Drücker, S.; Bettermann, S.; Schroeter, B.; Pauer, W.; Moritz, H.-U.; Fiedler, B.; Luinstra, G.; Smirnova, I. Smart reactors − Combining stimuli-responsive hydrogels and 3D printing. *Chem. Eng. J.* **2020**, *387*, 123413.

(9) Eckert, K. M.; Müller, S.; Luinstra, G. A.; Smirnova, I. Exploring pNIPAM lyogels: Experimental study on swelling equilibria in various organic solvents and mixtures, supported by COSMO-RS analysis. *Fluid Phase Equilib.* **2024**, *586*, 114182.

(10) Dong, L.; Jiang, H. Autonomous microfluidics with stimuli-responsive hydrogels. *Soft Matter* **2007**, *3* (10), 1223−1230.

(11) Wang, J.; Chen, Z.; Mauk, M.; Hong, K.-S.; Li, M.; Yang, S.; Bau, H. H. Self-actuated, thermo-responsive hydrogel valves for lab on a chip. *Biomed. Microdevices* **2005**, *7* (4), 313−322.

(12) Beebe, D. J.; Moore, J. S.; Bauer, J. M.; Yu, Q.; Liu, R. H.; Devadoss, C.; Jo, B. H. Functional hydrogel structures for autonomous flow control inside microfluidic channels. *Nature* **2000**, *404* (6778), 588−590.

(13) Osada, Y.; Okuzaki, H.; Hori, H. A polymer gel with electrically driven motility. *Nature* **1992**, *355* (6357), 242−244.

(14) Tanaka, T. Collapse of Gels and the Critical Endpoint. *Phys. Rev. Lett.* **1978**, *40* (12), 820−823.

(15) Richter, A.; Howitz, S.; Kuckling, D.; Arndt, K.-F. Influence of volume phase transition phenomena on the behavior of hydrogel-based valves. *Sens. Actuators, B* **2004**, *99* (2−3), 451−458.

(16) Richter, A.; Klatt, S.; Paschew, G.; Klenke, C. Micropumps operated by swelling and shrinking of temperature-sensitive hydrogels. *Lab Chip* **2009**, *9* (4), 613−618.

(17) Seo, J.; Wang, C.; Chang, S.; Park, J.; Kim, W. A hydrogel-driven microfluidic suction pump with a high flow rate. *Lab Chip* **2019**, *19* (10), 1790−1796.

(18) Li, M.; van Zee, M.; Goda, K.; Di Carlo, D. Size-based sorting of hydrogel droplets using inertial microfluidics. *Lab Chip* **2018**, *18* (17), 2575−2582.

(19) Arakawa, T.; Shirasaki, Y.; Aoki, T.; Funatsu, T.; Shoji, S. Three-dimensional sheath flow sorting microsystem using thermosensitive hydrogel. *Sens Actuators, A* **2007**, *135* (1), 99−105.

(20) Gargava, A.; Arya, C.; Raghavan, S. R. Smart Hydrogel-Based Valves Inspired by the Stomata in Plants. *ACS Appl. Mater. Interfaces* **2016**, *8* (28), 18430−18438.

(21) Schneider, H.-J. Logic-Gate Functions in Chemomechanical Materials. *ChemPhysChem* **2017**, *18* (17), 2306−2313.

(22) Ansari, M. J.; Rajendran, R. R.; Mohanto, S.; Agarwal, U.; Panda, K.; Dhotre, K.; Manne, R.; Deepak, A.; Zafar, A.; Yasir, M.; Pramanik, S. Poly(N-isopropylacrylamide)-Based Hydrogels for Biomedical Applications: A Review of the State-of-the-Art. *Gels* **2022**, *8* (7), 454.

(23) El-Sherbiny, I. M.; Yacoub, M. H. Hydrogel scaffolds for tissue engineering: Progress and challenges. *Global Cardiol. Sci. Pract.* **2013**, *2013* (3), 38.

(24) Kopecek, J. Hydrogel biomaterials: a smart future? *Biomaterials* **2007**, *28* (34), 5185−5192.

(25) Nagase, K.; Yamato, M.; Kanazawa, H.; Okano, T. Poly(N-isopropylacrylamide)-based thermoresponsive surfaces provide new types of biomedical applications. *Biomaterials* **2018**, *153*, 27−48.

(26) Parhi, R. Cross-Linked Hydrogel for Pharmaceutical Applications: A Review. *Adv. Pharm. Bull.* **2017**, *7* (4), 515−530.

(27) Vigata, M.; Meinert, C.; Hutmacher, D. W.; Bock, N. Hydrogels as Drug Delivery Systems: A Review of Current Characterization and Evaluation Techniques. *Pharmaceutics* **2020**, *12* (12), 1188.

(28) Khan, F.; Tanaka, M.; Ahmad, S. R. Fabrication of polymeric biomaterials: a strategy for tissue engineering and medical devices. *J. Mater. Chem. B* **2015**, *3* (42), 8224−8249.

(29) Banerjee, I.; Mishra, D.; Das, T.; Maiti, T. K. Wound pH-responsive sustained release of therapeutics from a poly(NIPAAm-co-AAc) hydrogel. *J. Biomater. Sci., Polym. Ed.* **2012**, *23* (1−4), 111−132.

(30) Argentiere, S.; Gigli, G.; Gerges, M. M. I.; Blasi, L. Smart microfluidics: The role of stimuli-responsive polymers in microfluidic devices. In *Advances in Microfluidics*; IntechOpen, 2012.

(31) Huang, G. Y.; Zhou, L. H.; Zhang, Q. C.; Chen, Y. M.; Sun, W.; Xu, F.; Lu, T. J. Microfluidic hydrogels for tissue engineering. *Biofabrication* **2011**, *3* (4), 012001.

(32) Tevlek, A.; Çetin, E. A. Smart hydrogels in Lab-on-a-Chip (LOC) applications. *React. Funct. Polym.* **2024**, *204*, 106023.

(33) Lee, M. Y.; Lee, E. S.; Ko, N. Y.; Kim, H. J.; Kim, D.-H.; Cha, G. D.; Koo, J. H. Emerging roles of hydrogels, organogels, and their hybrids in soft bioelectronics and bioplatforms. *Npj Biosens.* **2025**, *2* (1), 35.
(34) Aktas, N.; Alpaslan, D.; Dudu, T. E. Polymeric Organo-Hydrogels: Novel Biomaterials for Medical, Pharmaceutical, and Drug Delivery Platforms. *Front. Mater.* **2022**, *9*, 845700.
(35) Rekha Rout, S.; Manu, K. R.; Kaur, G.; Abishek, K. G.; Alsayari, A.; Wahab, S.; Kesharwani, P.; Dandela, R. Recent advances in drug delivery aspects using Organogel: Exploring a viscoelastic system as a platform for the next-generation therapeutics. *Eur. Polym. J.* **2024**, *214*, 113184.
(36) Hoff, K. L.; Eisenacher, M. Process Intensification Strategies for Esterification: Kinetic Modeling, Reactor Design, and Sustainable Applications. *Int. J. Mol. Sci.* **2025**, *26* (15), 7214.
(37) Raju, A.; Jothish, S.; Sakthivel, K.; Mishra, S.; Gana, R. J.; Kikushima, K.; Dohi, T.; Singh, F. V. Recent advances in metal-catalysed oxidation reactions. *R. Soc. Open Sci.* **2025**, *12* (1), 241215.
(38) Friebe, L.; Nuyken, O.; Obrecht, W. Neodymium-Based Ziegler/Natta Catalysts and their Application in Diene Polymerization. In *Neodymium based Ziegler catalysts—Fundamental chemistry* Advances in Polymer Science, Nuyken, O. Ed.; Springer, 2006; pp. 1—154. .
(39) Reichardt, C. Solvents and Solvent Effects: An Introduction. *Org. Process Res. Dev.* **2007**, *11* (1), 105—113.
(40) Chen, Z.; Wu, H.; Deng, X.; Wang, X. Green Synthesis of Polymers under Solvent-Free Conditions. In *Sustainable green chemistry in polymer research:Volume 2, Sustainable polymers and applications*, ACS Symposium Series, Cheng, H. N.; Gross, R. A., Eds.; American Chemical Society, 2023; Vol. *1451*, pp. 125—147. .
(41) Burrows, C. J.; Harper, J. B.; Sander, W.; Tantillo, D. J. Solvation Effects in Organic Chemistry. *J. Org. Chem.* **2022**, *87* (3), 1599—1601.
(42) Sheldon, R. A. The E factor 25 years on: the rise of green chemistry and sustainability. *Green Chem.* **2017**, *19* (1), 18—43.
(43) Gawande, M. B.; Bonifácio, V. D. B.; Luque, R.; Branco, P. S.; Varma, R. S. Solvent-free and catalysts-free chemistry: a benign pathway to sustainability. *ChemSusChem* **2014**, *7* (1), 24—44.
(44) Eckert, K. M.; Bonsen, J.; Hajnal, A.; Gmeiner, J.; Hasse, J.; Adrian, M.; Karsten, J.; Kißling, P. A.; Penn, A.; Fiedler, B.; Luinstra, G. A.; Smirnova, I. Enhancing swelling kinetics of pNIPAM lyogels: The role of crosslinking, copolymerization, and solvent. *Fluid Phase Equilib.* **2025**, *597*, 114462.
(45) Komarova, G. A.; Kozhunova, E. Y.; Potemkin, I. I. Behavior of PNIPAM Microgels in Different Organic Solvents. *Molecules* **2022**, *27* (23), 8549.
(46) Wu, Y.; Ke, Y.; Lin, T.; He, X.; Xu, J. Preparation and application of organic hydrogels incorporating polyacrylamide/sodium alginate/DMSO for enhanced anti-drying, anti-freezing, and self-healing properties. *Polymer* **2024**, *313*, 127693.
(47) Kuzina, M. A.; Kartsev, D. D.; Stratonovich, A. V.; Levkin, P. A. Organogels versus Hydrogels: Advantages, Challenges, and Applications. *Adv. Funct. Mater.* **2023**, *33* (27), 2301421.
(48) Chen, H.; Zhang, D.; Xiao, S.; Wu, J.; Wei, J.; Tang, Y.; Zhao, C.; Zheng, J. Organogels: Mechanistic insights, design strategies, and translational applications. *Prog. Mater. Sci.* **2026**, *158*, 101642.
(49) Alsaid, Y.; Wu, S.; Wu, D.; Du, Y.; Shi, L.; Khodambashi, R.; Rico, R.; Hua, M.; Yan, Y.; Zhao, Y.; Aukes, D.; He, X. Tunable Sponge-Like Hierarchically Porous Hydrogels with Simultaneously Enhanced Diffusivity and Mechanical Properties. *Adv. Mater.* **2021**, *33* (20), No. e2008235.
(50) Tanaka, T.; Fillmore, D. J. Kinetics of swelling of gels. *J. Chem. Phys.* **1979**, *70* (3), 1214—1218.
(51) Masaro, L.; Zhu, X. Physical models of diffusion for polymer solutions, gels and solids. *Prog. Polym. Sci.* **1999**, *24* (5), 731—775.
(52) Lee, E.; Lee, H.; Yoo, S. I.; Yoon, J. Photothermally triggered fast responding hydrogels incorporating a hydrophobic moiety for light-controlled microvalves. *ACS Appl. Mater. Interfaces* **2014**, *6* (19), 16949—16955.
(53) Haq, M. A.; Su, Y.; Wang, D. Mechanical properties of PNIPAM based hydrogels: A review. *Mater. Sci. Eng., C* **2017**, *70* (Pt 1), 842—855.
(54) Fortes, A. F.; Joseph, D. D.; Lundgren, T. S. Nonlinear mechanics of fluidization of beds of spherical particles. *J. Fluid Mech.* **1987**, *177*, 467—483.
(55) Distler, T.; Kretzschmar, L.; Schneidereit, D.; Girardo, S.; Goswami, R.; Friedrich, O.; Detsch, R.; Guck, J.; Boccaccini, A. R.; Budday, S. Mechanical properties of cell- and microgel bead-laden oxidized alginate-gelatin hydrogels. *Biomater. Sci.* **2021**, *9* (8), 3051—3068.
(56) Khanam, U. S.; Jeong, H. T.; Mutlu, R.; Aziz, S. Alginate Sphere-Based Soft Actuators. *Gels* **2025**, *11* (6), 432.
(57) Jurjevec, S.; Žagar, E.; Pahovnik, D.; Kovačič, S. Highly porous polyelectrolyte beads through multiple-emulsion-templating: Synthesis and organic solvent drying efficiency. *Polymer* **2021**, *212*, 123166.
(58) Ruckenstein, E. Sedimentation polymerization. *Polymer* **1995**, *36* (14), 2857—2860.
(59) Pahlavan, A. A.; Yang, L.; Bain, C. D.; Stone, H. A. Evaporation of Binary-Mixture Liquid Droplets: The Formation of Picoliter Pancakelike Shapes. *Phys. Rev. Lett.* **2021**, *127* (2), 24501.
(60) Okten, N. S.; Canakci, C. C.; Orakdogen, N. Hertzian elasticity and triggered swelling kinetics of poly(amino ester)-based gel beads with controlled hydrophilicity and functionality: A mild and convenient synthesis via dropwise freezing into cryogenic liquid. *Eur. Polym. J.* **2019**, *114*, 176—188.
(61) Salmerón Sánchez, M.; Monleón Pradas, M.; Gómez Ribelles, J. L. Thermal transitions in PHEA hydrogels by thermomechanical analysis. A comparison with DSC data. *Eur. Polym. J.* **2004**, *40* (2), 329—334.
(62) Kim, J. H.; Sim, S. J.; Lee, D. H.; Kim, D.; Lee, Y. K.; Chung, D. J.; Kim, J.-H. Preparation and Properties of PHEA/Chitosan Composite Hydrogel. *Polym. J.* **2004**, *36* (12), 943—948.
(63) Ferrer, G. G.; Pradas, M. M.; Gómez Ribelles, J. L.; Sánchez, M. S. Thermodynamical analysis of the hydrogel state in poly(2-hydroxyethyl acrylate). *Polymer* **2004**, *45* (18), 6207—6217.
(64) Serrano Aroca, A.; Gómez Ribelles, J. L.; Monleón Pradas, M.; Vidaurre Garayo, A.; Suay Antón, J. Characterisation of macroporous poly(methyl methacrylate) coated with plasma-polymerised poly(2-hydroxyethyl acrylate). *Eur. Polym. J.* **2007**, *43* (10), 4552—4564.
(65) Myung, D.; Koh, W.; Bakri, A.; Zhang, F.; Marshall, A.; Ko, J.; Noolandi, J.; Carrasco, M.; Cochran, J. R.; Frank, C. W.; Ta, C. N. Design and fabrication of an artificial cornea based on a photolithographically patterned hydrogel construct. *Biomed. Microdev.* **2007**, *9* (6), 911—922.
(66) Hoenle AG *LED Cube 100 IC* https://www.hoenle.com/products-solutions/product-categories/uv-curing-chambers/hoenle-led-cube-100-ic/ (accessed 2026—04—21).
(67) Hertz, H. Ueber die Berührung fester elastischer Körper. *J. Reine Angew. Math.* **1882**, *1882* (92), 156—171.
(68) Johnson, K. L. *Contact mechanics*; Cambridge University Press, 1985.
(69) Ryskulova, K.; Hou, Z.; Woisel, P.; Hoogenboom, R. Effect of Host-Guest Complexation on the Thermoresponsive Behavior of Poly(oligo ethylene glycol acrylate)s Functionalized with Dialkoxynapththalene Guest Side Chains. *Macromol. Rapid Commun.* **2021**, *42* (18), No. e2100068.
(70) Zhou, J.; Shi, D.; Kaneko, T.; Dong, W.; Chen, M. Regulating Electrostatic Interactions toward Thermoresponsive Hydrogels with Low Critical Solution Temperature. *Macromol. Rapid Commun.* **2024**, *45* (3), No. e2300488.
(71) Vargün, E.; Usanmaz, A. Polymerization of 2-hydroxyethyl acrylate in bulk and solution by chemical initiator and by ATRP method. *J. Polym. Sci., Part A: Polym. Chem.* **2005**, *43* (17), 3957—3965.
(72) Guan, M.; Wang, C.; Zhang, J.; Zhao, Y. Practical organic solvent-free Cu(OAc) 2/DMAP/TEMPO-catalyzed aldehyde and

https://doi.org/10.1021/acs.iecr.6c00936
Ind. Eng. Chem. Res. XXXX, XXX, XXX—XXX

imine formation from alcohols under air atmosphere. *RSC Adv.* **2014**, *4* (90), 48777−48782.
(73) van Krevelen, D. W. *Properties Of polymers: Their Correlation With Chemical Structure; Their Numerical Estimation And Prediction From Additive Group Contributions*; Elsevier, 2009.
(74) Hansen, C. M. *Hansen solubility parameters:A user's handbook*; CRC Press, 2007.
(75) Ahmed, E. M. Hydrogel: Preparation, characterization, and applications: A review. *J. Adv. Res.* **2015**, *6* (2), 105−121.
(76) Li, X.; Liu, X.; Chen, Q.; Wang, Y.; Feng, Y. Hydrophobically Associating Polyacrylamides Prepared by Inverse Suspension Polymerization: Synthesis, Characterization and Aqueous Solution Properties. *J. Macromol. Sci., Part A* **2010**, *47* (4), 358−367.
(77) Vaziri, A.; Maia, R.; Zhang, P.; Agresti, L.; Sjollema, J.; Shahbazi, M.-A.; Santos, H. A. Granular Hydrogels as Modular Biomaterials: From Structural Design to Biological Responses. *Adv. Healthcare Mater.* **2026**, *15* (3), No. e02462.
(78) Daly, A. C.; Riley, L.; Segura, T.; Burdick, J. A. Hydrogel microparticles for biomedical applications. *Nat. Rev. Mater.* **2020**, *5* (1), 20−43.
(79) Hernández, J. R.; Pradas, M. M.; Ribelles, J. G. Properties of poly(2-hydroxyethyl acrylate)-silica nanocomposites obtained by the sol−gel process. *J. Non-Cryst. Solids* **2008**, *354* (17), 1900−1908.
(80) Dušek, K. Diffusion control in the kinetics of cross-linking. *Polym. Gels Networks* **1996**, *4* (5−6), 383−404.
(81) *Physics of polymer gels*, Sakai, T., Ed.; Wiley-VCH, 2020.
(82) Das, A.; Babu, A.; Chakraborty, S.; van Guyse, J. F. R.; Hoogenboom, R.; Maji, S. Poly(N-isopropylacrylamide) and Its Copolymers: A Review on Recent Advances in the Areas of Sensing and Biosensing. *Adv. Funct. Mater.* **2024**, *34* (37), 2402432.
(83) Bharadwaj, S.; Niebuur, B.-J.; Nothdurft, K.; Richtering, W.; van der Vegt, N. F. A.; Papadakis, C. M. Cononsolvency of thermoresponsive polymers: where we are now and where we are going. *Soft Matter* **2022**, *18* (15), 2884−2909.
(84) Nikitin, A. N.; Hutchinson, R. A.; Buback, M.; Hesse, P. Determination of Intramolecular Chain Transfer and Midchain Radical Propagation Rate Coefficients for Butyl Acrylate by Pulsed Laser Polymerization. *Macromolecules* **2007**, *40* (24), 8631−8641.
(85) Plessis, C.; Arzamendi, G.; Leiza, J. R.; Schoonbrood, H. A. S.; Charmot, D.; Asua, J. M. Seeded Semibatch Emulsion Polymerization of n -Butyl Acrylate. Kinetics and Structural Properties. *Macromolecules* **2000**, *33* (14), 5041−5047.
(86) Gmeiner, J.; Hasse, J.; Eckert, K. M.; Smirnova, I.; Luinstra, G. A. *Organogel Beads by UV-Droplet Polymerization; Kinetic Study of their Chemoresponsiveness*. TUHH. 2026.
(87) Nothdurft, K.; Müller, D. H.; Mürtz, S. D.; Meyer, A. A.; Guerzoni, L. P. B.; Jans, A.; Kühne, A. J. C.; De Laporte, L.; Brands, T.; Bardow, A.; et al. Is the Microgel Collapse a Two-Step Process? Exploiting Cononsolvency to Probe the Collapse Dynamics of Poly-N-isopropylacrylamide (pNIPAM). *J. Phys. Chem. B* **2021**, *125* (5), 1503−1512.
(88) Jiang, Y.; Zeng, F.; Gong, R.; Guo, Z.; Chen, C.-F.; Wan, X. A multi-stimuli responsive organogel based on a tetrapeptide−dithienylcyclopentene conjugate. *Soft Matter* **2013**, *9* (31), 7538.

https://doi.org/10.1021/acs.iecr.6c00936
Ind. Eng. Chem. Res. XXXX, XXX, XXX−XXX